Opto-Electronic Engineering
光 电 工 程

Article

2019 年，第 46 卷，第 8 期

DOI: 10.12086/oee.2019.180577

二维光子晶体双重亚波长成像

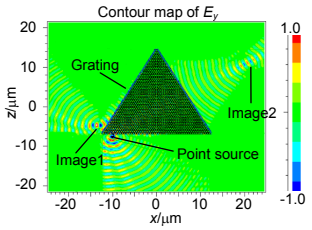

牛金科，梁斌明*，庄松林，陈家璧

上海理工大学光电信息与计算机工程学院，上海 200093

摘要：本文基于硅基底空气孔型二维光子晶体(photonic crystals)，提出了一种可以实现等效负折射和亚波长成像的结构。点光源通过三角形光子晶体出射后在两侧形成两个像点。通过在光子晶体两侧添加光栅，增加了光源的透过率，消除了旁斑对双重像点的影响。当光栅的空气带隙宽度 w=0.76a 和到光子晶体的距离 d_g=0.1a 时，左侧像点 image1 的最小半宽度达到 0.433λ，此时右侧像点 image2 达到 0.842λ，均小于入射波长。另外，当光源波长在 3.19a 到 3.26a 范围内时，光子晶体可以实现宽光谱的双重亚波长成像。最后，根据点光源和双重像点的位置变化，求出了关于其坐标 x, z 的相对关系。

关键词：光子晶体；负折射；双重成像；亚波长成像；共聚焦

中图分类号：O734；TH74　　**文献标志码：**A

引用格式：牛金科，梁斌明，庄松林，等. 二维光子晶体双重亚波长成像[J]. 光电工程，2019，**46**(8): 180577

Dual subwavelength imaging based on two-dimensional photonic crystals

Niu Jinke, Liang Binming*, Zhuang Songlin, Chen Jiabi

School of Optical-Electrical and Computer Engineering, University of Shanghai for Science and Technology, Shanghai 200093, China

Abstract: A focusing structure which can achieve negative refraction and dual subwavelength imaging is proposed, which is based on two-dimensional (2D) photonic crystal (PC) which consisting of air holes in silicon. The light radiated from a point source can form two images through a triangular PC. The transmittance of light is increased and the side spot at image2 is eliminated by adding the gratings on the sides of the PC. When the air slit of gratings is w=0.76a and the distance between gratings and PC is d_g=0.1a, the minimum half-width of the image1 reaches 0.433λ, the maximum half-width of image2 reaches 0.842λ, which are both lower than incident wavelength. In addition, the PC realizes wide-spectrum dual subwavelength imaging when the incident wavelength varies from 3.19a to 3.26a. The position formulas between images and point source are also demonstrated. Based on the results, we propose a new confocal system based on PC that can achieve subwavelength imaging.

Keywords: photonic crystals; negative refraction; dual imaging; subwavelength imaging; confocal

Citation: Niu J K, Liang B M, Zhuang S L, *et al.* Dual subwavelength imaging based on two-dimensional photonic crystals[J]. *Opto-Electronic Engineering*, 2019, **46**(8): 180577

收稿日期：2018-11-12； 收到修改稿日期：2019-01-07

基金项目：国家自然科学基金资助项目(61177043)

作者简介：牛金科(1992-)，男，硕士，主要从事光子晶体亚波长成像器件的研究。E-mail：976325867@qq.com

通信作者：梁斌明(1977-)，男，博士，副教授，主要从事微纳光学的研究。E-mail：bmliang78@aliyun.com

1 引 言

近年来，负折射率(negative refractive index)材料因具有亚波长成像和反常 Doppler 效应等特性吸引了越来越多的关注和研究[1-5]。截至目前，科学家已经提出了多种具有这些性质的负折射材料，常见的有周期排列金属谐振腔与细线结构[6]和光子晶体(photonic crystals，PC)[7]。光子晶体是一种新型的光学微结构材料，它为一种周期性排列的无损介质阵列，可有效控制光子的传播行为。相比金属结构，光子晶体在更高频率和更短波长时损耗较小[7-10]。由于能够在传播的过程中放大倏逝波，光子晶体可以突破衍射极限，实现超分辨成像[11-13]。Li 等人[14]通过光子晶体实现了高质量的近场成像。Zheng 等人[15]也通过石墨烯等材料实现了三维的亚波长成像。此外，光子晶体在亚波长光刻[16]、电光偏转器[17]和光子晶体光纤[18]等领域也吸引了广泛研究。同时，自 1957 年共焦激光显微镜问世以来，它以低噪声，高光强等特点推动了科学尤其是生命科学的巨大进步[19-22]。本文提出了一种基于二维光子晶体的负折射结构，通过在光子晶体两侧添加光栅增加光的透过，消除反射光形成的旁斑对双重成像的影响，得到清晰的双重亚波长像点。基于双重像点和光源之间的位置关系，本文提出了一种以三角形光子晶体为主要结构的共聚焦系统，与传统的共聚焦系统通过反射光再聚焦不同，该共聚焦系统结构简单，其聚焦成像通过光子晶体的负折射实现。

2 理论推导

文中使用基于硅基底空气孔型的二维光子晶体，其中硅材料的折射率为 3.45，空气的折射率为 1。光子晶体晶格常数 a 为 0.482 μm，空气孔的半径为 r=0.4015a。文中选用 TE 偏振光源，其工作频率ω对应的波长为λ=3.216a，根据平面波展开法求出的 TE 偏振光第一光子带中等频面(equal frequency surface，EFS)如图 1 所示。

图 1 显示，等频率曲线的值由外向内逐渐增加，波矢 $\boldsymbol{k}$ 的值由等频图中心向外增大，此时群速度与相速度相反，表示在此波长范围内折射率为负值。文中选取工作波长λ=0.3112×2πc/a，其中 c 为光在真空中的速度，在等频图中对应的波矢 $\boldsymbol{k}$ 为 4.06 rad/m。根据波矢大小 $\boldsymbol{k}$ 和归一化频率 f 的计算公式：

$$\boldsymbol{k}=\frac{\omega}{c}n_{\text{eff}} \quad , \tag{1}$$

$$f=\frac{\omega a}{2\pi c}=\frac{a}{\lambda} \quad , \tag{2}$$

得出等效折射率 $n_{\text{eff}}=\boldsymbol{k}\lambda/2\pi\approx1.002$，此时光子晶体对应的等效折射率约为-1。

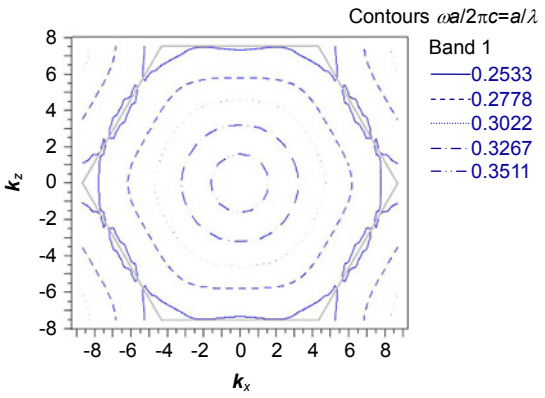

图 1 光子晶体第一 TE 偏振光子带等频面图

Fig. 1 Several EFS contours in the first TE-polarized photonic band of the PC

3 仿真结果

光子晶体的边长 L=50a，图 2 为光子晶体边缘基于硅基底的表面亚波长光栅结构。设置光栅 h_1=0.5015a，h_2=0.9615a，光栅厚度则为 h_2−h_1=0.46a，图中 d=0.8r 为底层空气柱圆心到光子晶体边缘的距离，此时光栅到光子晶体表面空气柱的距离 d_g=h_1−r=0.1a。点光源位于光子晶体下表面 0.3 μm 处，其横向坐标为-10 μm。由于 TE 波在平面光波导中电磁场没有 E_x 分量，根据光路仿真软件 Rsoft 模拟得到的 E_y 分量传播图如图 3 所示，可明显看出，相比于图 3(a)，添加光栅后的图 3(b)具有更好的成像效果。

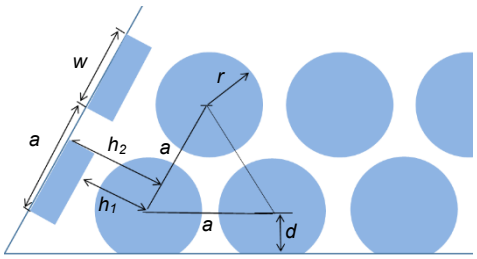

图 2 等边三角形光子晶体变量示意图

Fig. 2 Variable schematic diagram on an enlarged equilateral triangle PC

仿真模拟中光源的强度为 2 a.u，图 3(c)和图 3(d)分别是光子晶体左右两侧的探测器能量输出值，它们归一化输出值的范围为[0，2]。根据图 3(c)可知，图 3(a)中 image1 的峰值小于图 3(b)中 image1 的峰值。

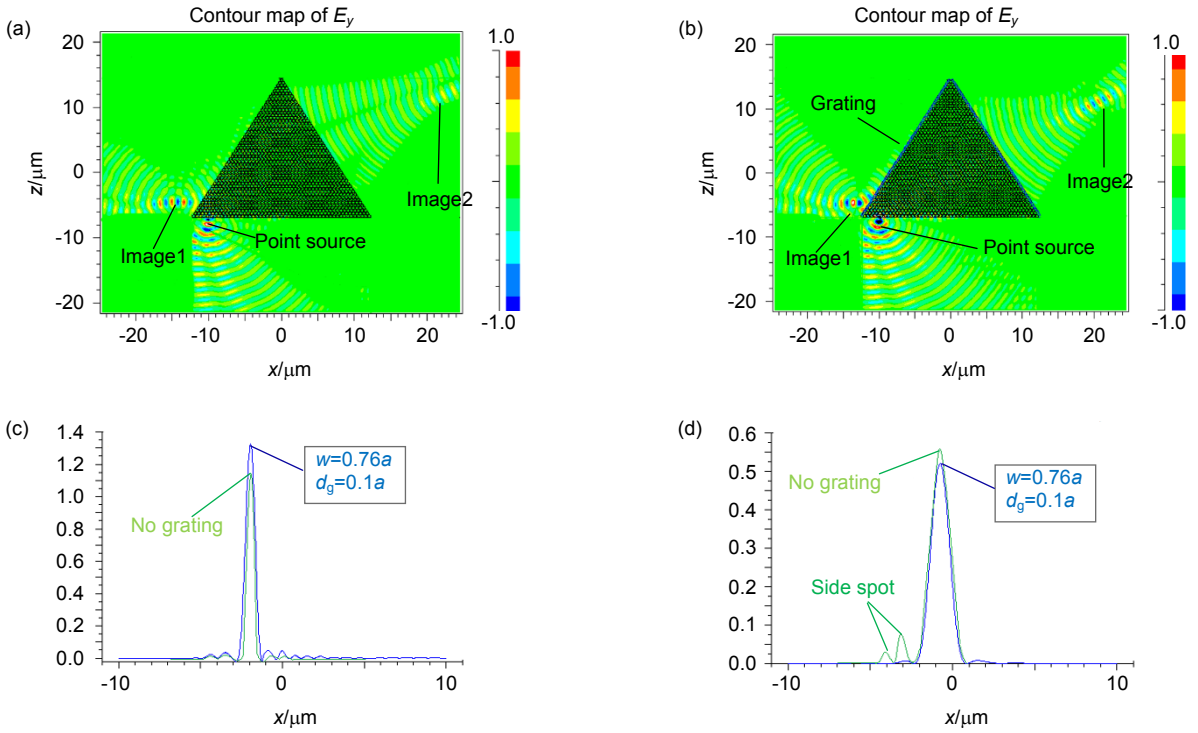

图 3 无光栅和有光栅时光子晶体负折射和亚波长双重成像，其中 λ=3.216a 光源位于光子晶体下表面 0.3 μm 处，其横坐标为 x=-10 μm。(a) 无光栅时光路图；(b) 有光栅时光路图；(c) 无光栅和有光栅时 image1 处的能量探测器输出值；(d) 无光栅和有光栅时 image2 处的能量探测器输出值

Fig. 3 Negative refraction and dual subwavelength imaging of the point source through the equilateral triangle PC without grating and gratings λ=3.216a, the point source is located at 0.3 μm below the PC, and its horizontal coordinate is x=-10 μm. (a) No grating; (b) With gratings; (c) Output values of two energy detectors at the image1 when no grating and with gratings; (d) Output values of two energy detectors at the image2 when no grating and with gratings

image2 处探测器的输出值如图 3(d)所示，由于来自光子晶体左侧的反射光的影响，图 3(a)中 image2 的峰值大于图 3(b)中 image2 的峰值，且存在旁斑。在光子晶体侧边添加光栅后，由于增加了光子晶体透射率，反射光对 image2 的影响明显减小。由于 image2 的干扰主要来自左侧的反射，则左侧透过越大，到右侧的反射越小，因此我们以 image1 为研究对象，讨论光栅宽度和相对位置对成像的影响。

4 数据分析

亚波长光栅等价于抗反射薄膜，能增强光能量透射，且透射波的波阵面不发生改变。可以通过调节光栅空气带隙和光栅与光子晶体的相对距离，改变亚波长光栅在光子晶体表面的抗反射效果。变量 w 是光栅中空气带隙的宽度，d_g 为光栅到光子晶体表面空气柱的距离，通过调节 w 和 d_g 改变光子晶体透镜能量的透射率。

仿真结果表明，光栅空气孔带隙的宽度确实可以提高成像质量。根据不同的 w 和 d_g 所对应的探测器结果，得出折线图如图 4(a)和 4(b)所示。

图 4(a)显示在 w=0.76a 时 image1 取得最大的峰值。image1 的峰值从无光栅的 1.104 增加到 w=0.76a 时的 1.324，半宽度从 0.461λ 减小到 0.433λ；同时，当光栅 w=0.76a 时，反射光对 image2 的影响减小，此时 image2 的归一化峰值为 0.521，半宽度为 0.842λ。

图 4(b)为光栅相对光子晶体不同距离时 image1 的峰值和半宽变化曲线，从图中可知，在 d_g 为 0.1a 时点光源取得最大的透过率且 image1 达到最小半宽。在 w=0.76a 和 d_g=0.1a 时，光源取得最高的能量透过。因此，选择在 w=0.76a 和 d_g=0.1a 来做后续的仿真。考虑到入射波长稍有偏差，成像也产生一定的偏差，通过改变入射波长变化来模拟入射光波长对成像的影响。

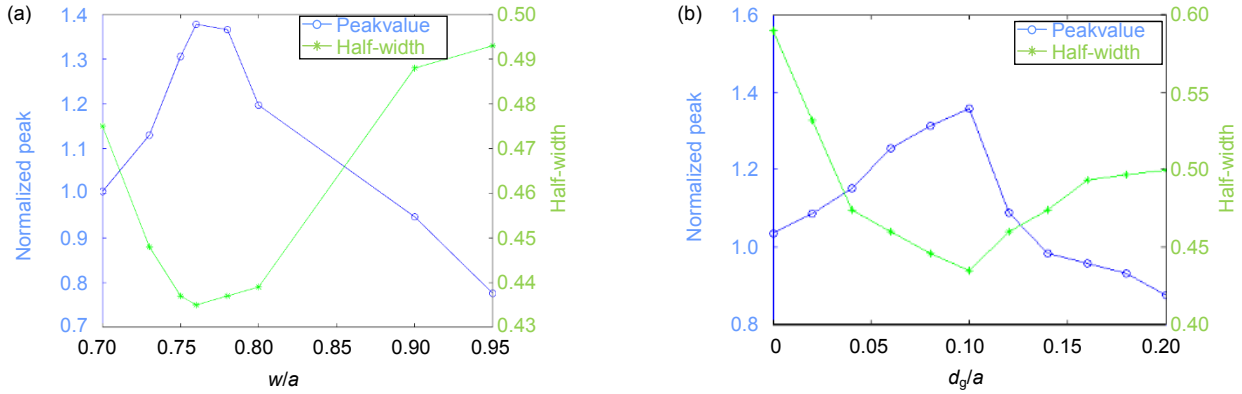

图 4 Image1 的半宽度和峰值随(a) w 和(b) d_g 的变化

Fig. 4 The half-width and peak value of image1 various with (a) w and (b) d_g

图 5 显示了双重像点的半宽度随入射波长的变化，当点光源的入射波长为 3.216a 时，image1 的最小半宽度约为 0.433λ，image2 的半宽度在整个波长区间单调减小。当入射波长在 3.19a 到 3.26a 之间时，image1 的半宽度小于 0.44λ，image2 的半宽度也稳定在 0.83λ 左右，这意味着光子晶体可以在这个范围内实现稳定的宽光谱双重亚波长成像。

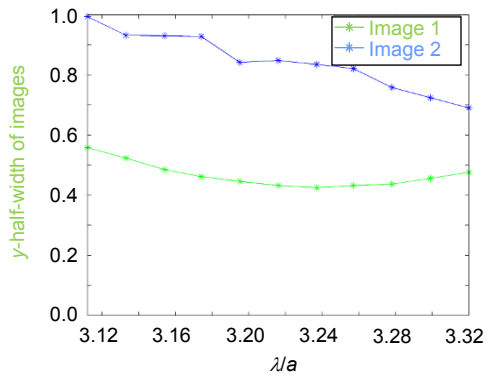

图 5 当点光源波长从 3.11a 到 3.32a 时像点的半宽变化

Fig. 5 The half-width of the images when the wavelength of point source from 3.11a to 3.32a

接下来，为了分析点光源的位置对双重成像的影响，将点光源的水平位置从 0 μm 移动到-10 μm，在不改变其他参数的情况下模拟光路，然后绘制半宽度折线图如图 6(a)所示。由图 6(a)可知，随着点光源向左移动，image1 的半宽度不断减小，image2 的半宽度单调增加。由于光子晶体结构是对称的，当点光源位于光子晶体下边缘的中点(x=0)时，image1 和 image2 的半宽度相等。

随着点光源的移动，像点的半宽总是小于入射波长。图 6(b)中展示了像点的位置随点光源横坐标的变化，红色箭头表示其运动方向，可以看出当点源的水平坐标从 0 到-10 μm 变化时，两侧的像点沿直线移动。其中 image1 移动了 10.6 μm，image2 移动 6.8 μm。得出点光源的水平位置与像点坐标 x、z 的关系公式，image1 为

$$x_1 = 0.58|x| - 18.7\ ,\quad z_1 = -0.89|x| + 4.3\ ;$$

image2 是

$$x_2 = 0.2|x| + 18.7\ ,\quad z_2 = 0.65|x| + 4.3\ ,$$

其中 x 是点光源的水平坐标。

根据以上结果和光路的可逆性，提出了基于三角形二维光子晶体的共聚焦系统，其光路如图 7(a)所示。为了保证激光聚焦在物体所在的焦平面上，且激光激发的荧光在探测针孔中能够更好地成像，将物体置于光子晶体透镜的中点。模拟使用 He-Ne 激光器的激发波长λ_1=543 nm，荧光染料的发射波长λ_2=585 nm，为了保证其等效折射率为-1，光子晶体的晶格常数设为 0.169 μm。

探测针孔和点光源始终汇聚在同一焦点上，使焦平面外激发的荧光不能进入探测针孔。还可以在像点前设置二向色镜来减少激光光源的影响。激发光(激光)的聚焦过程和发射光(荧光)的成像过程分别如图 7(b)和图 7(c)所示，测量的物体焦点的半宽是 0.54λ_1，像点的半宽为 0.51λ_2。结果表明，在该方法中可以实现共聚焦亚波长成像。与传统的共聚焦系统相比，这种共聚焦结构不需要物镜，聚焦和成像通过光子晶体的负折射实现，其结构更加简单。

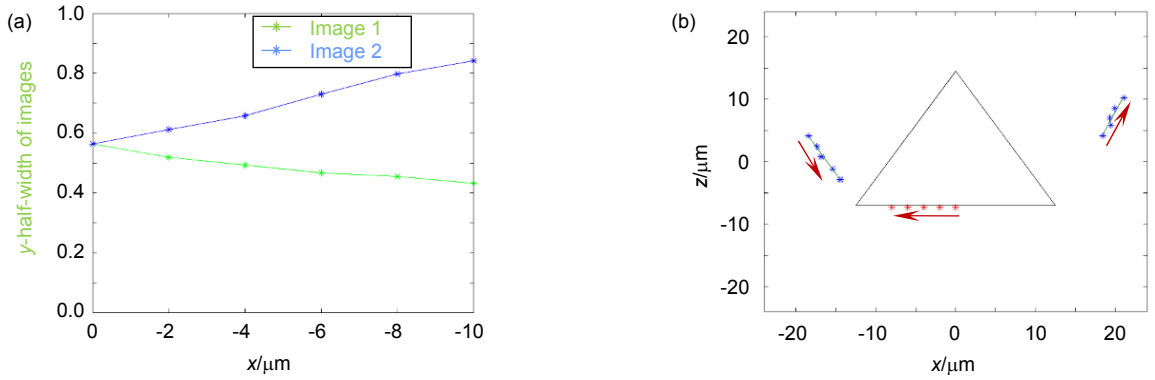

图 6　点光源从 0 移动到-10 μm。(a) 两像点半宽变化；(b) 两像点的位置变化

Fig. 6　Point source moves from 0 to -10 μm. (a) The half-width of images; (b) Position of images

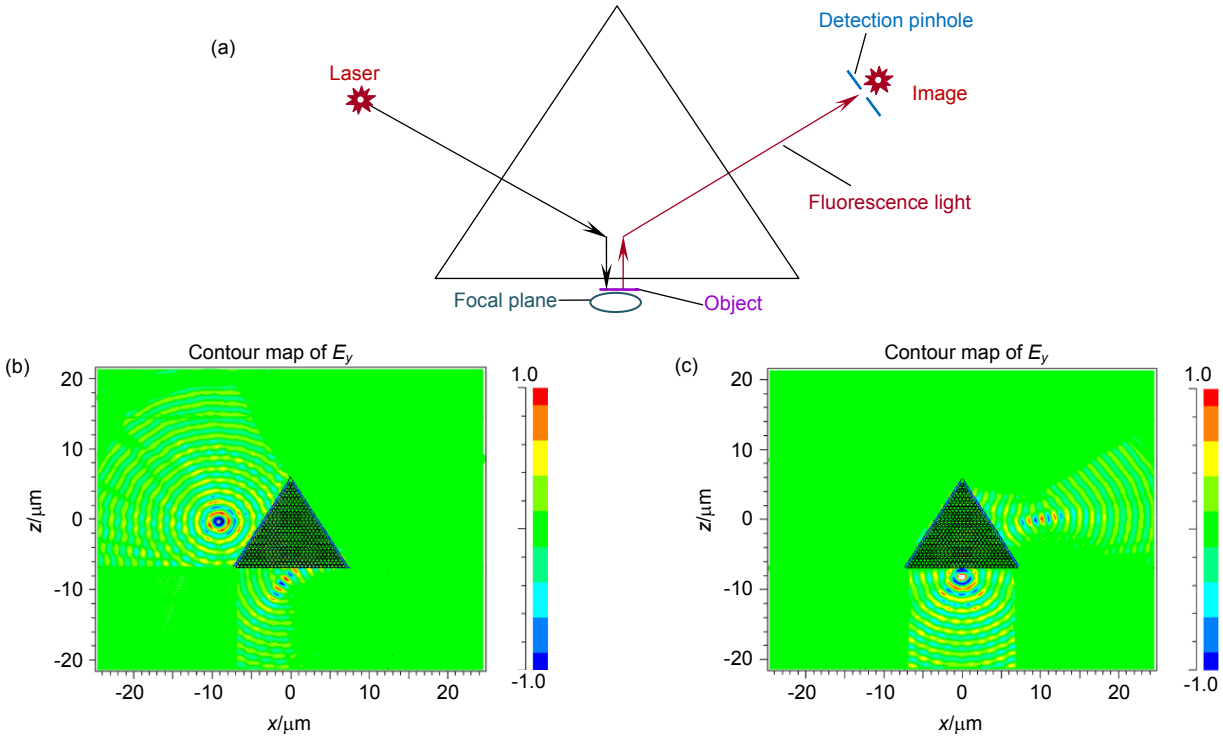

图 7　光子晶体共聚焦系统。(a) 共聚焦示意图；(b) 激光激发路径；(c) 荧光反射路径

Fig. 7　Confocal system based on PC. (a) Confocal diagram; (b) Path of laser; (c) Path of fluorescence

5　结　论

本文提出了一种可以实现负折射和双重亚波长成像的光子晶体结构。通过调整光栅间隙大小和相对位置，image1 的归一化峰值从 1.104 增加到 1.326，半宽度从 0.461λ 减小到 0.433λ；同时，当光栅空气狭缝 w=0.76a，光栅到光子晶体空气孔距离 d_g=0.1a 时，image2 处的旁斑消失。当入射波长为 3.216a 时获得最小半宽度的像点，并且当入射波长在 3.19a 到 3.26a 之间时可以实现宽光谱双重亚波长成像，其中最小半宽度小于 0.44λ。此外，文中还得出了像点和点光源的位置公式，为双重像点的精确定位提供了参考。在此基础上，提出了一种可以实现亚波长成像的共聚焦系统，与传统的共聚焦系统相比，这种结构不需要物镜，其聚焦和成像通过光子晶体的负折射实现，结构更加简单。除此之外，双重亚波长成像在激光光刻等其他方面也有很好的应用前景。

参考文献

[1] Veselago V G. The electrodynamics of substances with simultaneously negative values of ε and μ[J]. *Soviet Physics Uspekhi*, 1968, **10**(4): 509.

[2] Pendry J B. Negative refraction makes a perfect lens[J]. *Physical Review Letters*, 2000, **85**(18): 3966–3969.

[3] Kang M, Chen J, Li S M, *et al*. Optical spin-dependent angular shift in structured metamaterials[J]. *Optics Letters*, 2011, **36**(19): 3942–3944.

[4] Iyer A K, Eleftheriades G V. Mechanisms of subdiffraction free-space imaging using a transmission-line metamaterial superlens: an experimental verification[J]. *Applied Physics Letters*, 2008, **92**(13): 131105.

[5] Shelby R A, Smith D R, Schultz S. Experimental verification of a negative index of refraction[J]. *Science*, 2001, **292**(5514): 77–79.

[6] Martín F, Bonache J, Falcone F, *et al*. Split ring resonator-based left-handed coplanar waveguide[J]. *Applied Physics Letters*, 2003, **83**(22): 4652–4654.

[7] Joannopoulos J D, Villeneuve P R, Fan S H. Photonic crystals: putting a new twist on light[J]. *Nature*, 1997, **386**(6621): 143–149.

[8] Mekis A, Chen J C, Kurland I, *et al*. High transmission through sharp bends in photonic crystal waveguides[J]. *Physical Review Letters*, 1996, **77**(18): 3787–3790.

[9] Notomi M. Theory of light propagation in strongly modulated photonic crystals: refractionlike behavior in the vicinity of the photonic band gap[J]. *Physical Review B*, 2000, **62**(16): 10696–10705.

[10] Engelen R J P, Sugimoto Y, Watanabe Y, *et al*. The effect of higher-order dispersion on slow light propagation in photonic crystal waveguides[J]. *Optics Express*, 2006, **14**(4): 1658–1672.

[11] Luo C Y, Johnson S, Joannopoulos J, *et al*. Subwavelength imaging in photonic crystals[J]. *Physical Review B*, 2003, **68**(4): 045115.

[12] Jiang L Y, Wu H, Li X Y. Dual-negative-refraction and imaging effects in normal two-dimensional photonic crystals with hexagonal lattices[J]. *Optics Letters*, 2012, **37**(11): 1829–1831.

[13] Cubukcu E, Aydin K, Ozbay E, *et al*. Subwavelength resolution in a two-dimensional photonic-crystal-based superlens[J]. *Physical Review Letters*, 2003, **91**(20): 207401.

[14] Li Z Y, Lin L L. Evaluation of lensing in photonic crystal slabs exhibiting negative refraction[J]. *Physical Review B*, 2003, **68**(24): 245110.

[15] Zheng X R, Jia B H, Lin H, *et al*. Highly efficient and ultra-broadband graphene oxide ultrathin lenses with three-dimensional subwavelength focusing[J]. *Nature Communications*, 2015, **6**: 8433.

[16] Li H Y, Wang C T, Luo X G. Planar hyper lens with demagnification for nanolithography[J]. *Opto-Electronic Engineering*, 2011, **38**(5): 35–39, 45.
李恒一, 王长涛, 罗先刚. 用于纳米光刻的超分辨缩小成像平板超透镜研究[J]. 光电工程, 2011, **38**(5): 35–39, 45.

[17] Gao L, Liang B M, Wang T, *et al*. Electro-optic deflector based on negative refraction effect of photonic crystal[J]. *Opto-Electronic Engineering*, 2016, **43**(5): 77–81.
高伦, 梁斌明, 王婷, 等. 光子晶体负折射效应的电光偏转器[J]. 光电工程, 2016, **43**(5): 77–81.

[18] Zhang X D, Yuan M M, Chang M, *et al*. Characteristics in square air hole structure photonic crystal fiber[J]. *Opto-Electronic Engineering*, 2018, **45**(5): 20–28.
张学典, 袁曼曼, 常敏, 等. 正方形空气孔光子晶体光纤特性分析[J]. 光电工程, 2018, **45**(5): 20–28.

[19] White J G, Amos W B. Confocal microscopy comes of age[J]. *Nature*, 1987, **328**(6126): 183–184.

[20] Minsky M. Memoir on inventing the confocal scanning microscope[J]. *Scanning*, 1988, **10**(4): 128–138.

[21] Egger M D. The development of confocal microscopy[J]. *Trends in Neurosciences*, 1989, **12**(1): 11.

[22] Ziegler D, Papanas N, Zhivov A, *et al*. Early detection of nerve fiber loss by corneal confocal microscopy and skin biopsy in recently diagnosed type 2 diabetes[J]. *Diabetes*, 2014, **63**(7): 2454–2463.

Dual subwavelength imaging based on two-dimensional photonic crystals

Niu Jinke, Liang Binming*, Zhuang Songlin, Chen Jiabi

School of Optical-Electrical and Computer Engineering, University of Shanghai for Science and Technology, Shanghai 200093, China

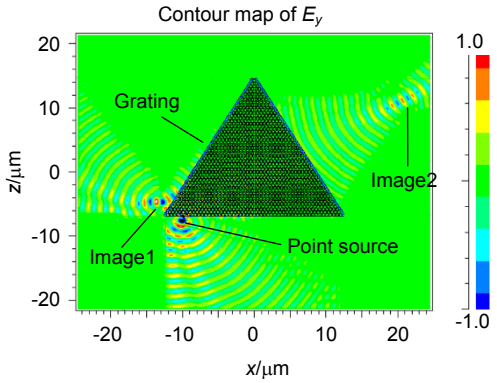

Negative refraction and dual subwavelength imaging of the point source through the equilateral triangle PC without grating and gratings λ=3.216a, the point source is located at 0.3 μm below the PC, and its horizontal coordinate is x=-10 μm

Overview: In recent years, negative refractive index materials (NIMs) have attracted more attention. There are lots of studies on the special characteristics of NIMs such as negative refraction and subwavelength imaging. As a NIM, photonic crystal (PC) can greatly amplify the evanescent waves and break the diffraction limit, the subwavelength resolution can be achieved.

In this paper, The edge length of PC is L=50a. The point source is placed at 0.3 μm below the edge of PC, and its horizontal coordinate is -10 μm. The light path simulated by Rsoft software. The gratings on both sides of the PC increases the transmission of light, eliminating the influence of the reflected light on dual imaging. As the clear two images are achieved, the positional relationship between two images and the point source is obtained. Based on the results, a confocal system with a triangular PC is proposed. Unlike the conventional confocal system, the PC confocal system has a simple structure, and it achieves imaging by negative refraction.

Dual sub-wavelength imaging is achieved clearly by adjusting the grating gap on PC, it eliminates the effects of reflected light. Through varying the wavelength of the point source, a broad spectrum which can achieve sub-wavelength imaging is found. Then adjust the lateral coordinates of the light source points to obtain the positional relationship between the two image points and the light source points. Based on the above results, the photonic crystal confocal system was designed and verified by simulation. The normalized peak value of image1 is increased from 1.104 to 1.326 and the half-width is decreased from 0.461λ to 0.433λ by adjusting the size of the grating air slit; meanwhile, the side spot at image2 is eliminated when the grating air slit is w=0.76a and distance between gratings and air hole is d_g=0.1a. The minimum half-width of images is obtained when the incident wavelength is 3.216a, and the wide-spectrum dual subwavelength imaging is achieved when the incident wavelength varies from 3.19a to 3.26 a, which the minimum half-width is less than 0.44λ. In addition, the position formulas of the images and point source are demonstrated, that provides a reference for the precise location of two images. Based on the results, we propose a confocal system that can achieve subwavelength imaging. Compared with the traditional confocal microscope, this structure does not need objective lens. As its focusing and imaging through the negative refraction of PC, the structure is more simple. Furthermore, dual subwavelength imaging can also be used in other aspects.

Citation: Niu J K, Liang B M, Zhuang S L, *et al*. Dual subwavelength imaging based on two-dimensional photonic crystals[J]. *Opto-Electronic Engineering*, 2019, **46**(8): 180577

Supported by National Natural Science Foundation of China (61177043)

* E-mail: bmliang78@aliyun.com